Asian Journal of Green Chemistry 10 (2026) 372-388

Asian Journal of Green Chemistry

Original Research Article View Article Online | View Journal

Eco-Friendly Waste-to-Resource Synthesis of Hydroxyapatite/Polyethylene Glycol Composites from Gonggong Clam Shells for Efficient Rhodamine B Dye Removal

Novesar Jamarun[1,*], Zulhadjri[1], Upita Septiani[1], Vivi Sisca[2], Arika Prasejati[1], Cynthia[1], Nabiila Ayyu Trycahyani[1], Adam Hidayat[1]

[1]*Department of Chemistry, Faculty of Mathematics and Natural Sciences, Andalas University, Padang, Indonesia*
[2]*Research Center for Chemistry, National Research and Innovation Agency (BRIN), South Tangerang, Indonesia*

ARTICLE INFORMATION

Submitted: 2025-09-01
Revised: 2025-10-15
Accepted: 2025-10-27
Published: 2025-10-30
Manuscript ID: AJGC-2509-1840
DOI: 10.48309/AJGC.2026.550310.1840

KEYWORDS

Gonggong shells
Composite
Hydroxyapatite
Polyethylene glycol
Rhodamine B

ABSTRACT

Dye waste is an environmental problem that requires an effective solution. One approach involves the use of adsorbent materials based on hydroxyapatite-polyethylene glycol (HAp/PEG) composites. In this study, HAp/PEG composites were synthesized using the in-situ sol-gel method with gonggong clam shell waste (*Laevistrombus canarium*) as a calcium source. The addition of polyethylene glycol (PEG) aimed to improve the porosity, dispersibility, and mechanical stability of hydroxyapatite (HAp). The characterization results confirmed the presence of typical HAp functional groups through Fourier transform infrared spectroscopy (FTIR), high crystallinity based on X-ray diffraction (XRD), a surface area of 73.001 m^2/g obtained from Brunauer-Emmett-Teller (BET) analysis, and irregular spherical morphology with a smooth surface as observed by field emission scanning electron microscopy coupled with energy-dispersive X-ray spectroscopy (FESEM–EDS). The Rhodamine B (RhB) adsorption tests showed optimal conditions at pH 11, with an adsorbent mass of 0.15 g, an initial concentration of 20 mg/L, and a contact time of 120 min. The adsorption process followed the Langmuir isotherm model and pseudo-second-order kinetics, yielding a maximum adsorption capacity of 3.19 mg/g. The HAp/PEG composite could be reused up to four cycles. In conclusion, the HAp/PEG composite derived from gonggong clam shell waste demonstrated strong potential as an efficient and eco-friendly adsorbent for Rhodamine B removal from wastewater.

Corresponding author, E-mail: novesarjamarun@sci.unand.ac.id (N. Jamarun).
Tel.: +08126713521.

Graphical Abstract

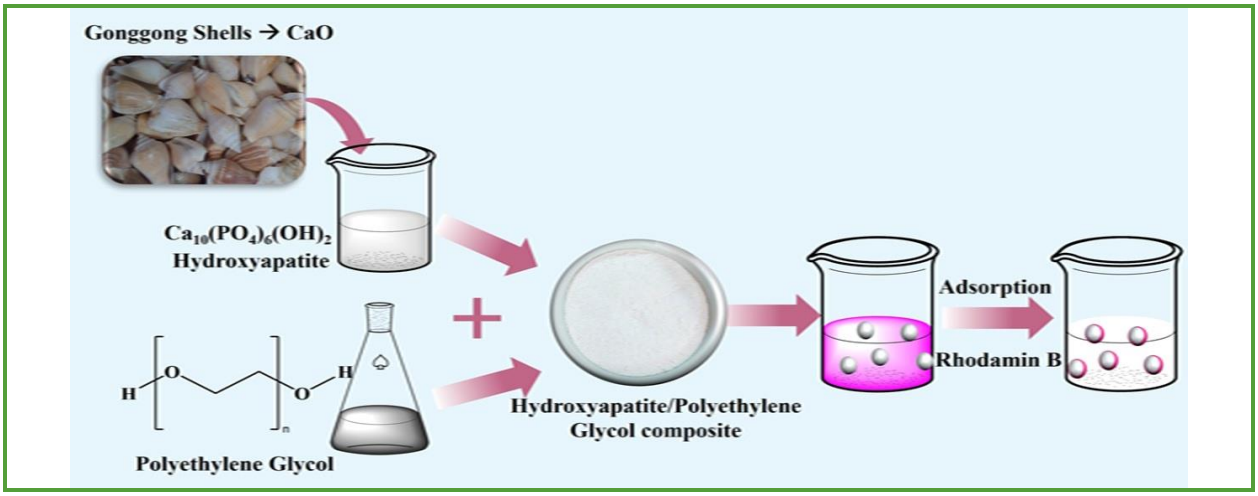

Introduction

Environmental pollution is a global issue described as introducing foreign chemicals or energy into ecosystems, disturbing the equilibrium, and endangering living species [1]. Water, air, soil, and biological pollution are the most common forms, and heavy metals, synthetic colors, pesticides, and toxic, non-biodegradable pharmaceutical residues are significant sources of concern [2,3]. Several techniques have been developed for preventing pollution, including membrane filtration, adsorption, coagulation, precipitation, and oxidation. Adsorption is deemed better among these approaches due to its low cost, simple procedure, possible regeneration, and high effectiveness in pollutant removal [4,5]. One effective adsorbent is hydroxyapatite (HAp), which is known for its thermal stability, biocompatibility, and high adsorption capacity for heavy metals and organic substances. HAp can be synthesized from environmentally friendly natural materials, including calcium-rich sources such as eggshells [6], mussel shells [7], blood cockle shells [8], and cuttlefish bones [9]. Additionally, gonggong shells (*Laevistrombus canarium*.) hold potential as precursors for HAp synthesis and can enhance the economic value of these shells. Despite HAp's promising performance as an adsorbent, its high surface reactivity often leads to particle agglomeration in solution, which reduces both the active surface area and the adsorption efficiency for pollutants [10]. To address this limitation, modifications were made by combining HAp with polymers, such as polyethylene glycol (PEG). PEG is a biocompatible, flexible, hydrophilic, and non-toxic polymer. It enhances the porosity, dispersibility, and mechanical stability of composite materials. However, PEG has the drawback of low thermal conductivity. Therefore, combining PEG with HAp aims to merge the advantages of both materials, resulting in a composite that has the potential to be used as an adsorbent material with high porosity and surface area [11]. Prior research showed successful in-situ synthesis of a hydroxyapatite/chitosan composite, which improved the adsorption efficiency of rhodamine B dye [12]. The optimal ratio for forming the HAp/PEG composite is 70:30, balancing the adsorption capacity of HAp with the mechanical properties of PEG. Previous studies by Jamarun, Trycahyani, *et al.* (2023)

demonstrated that using calcium oxide derived from blood clam shells produced a 70:30 HAp/PEG composite with nano-sized crystals, needle-like morphology, and an ideal calcium-to-phosphorus (Ca/P) ratio, showing excellent degradation and stability performance [13].

Recent studies have explored using biomass waste and natural materials as precursors for environmentally friendly materials in adsorption and catalysis applications. For instance, activated carbon synthesized from coconut husks through hydrothermal carbonization demonstrates high adsorption activity for methylene blue [14].

Biomass-based catalysts derived from eggshells and palm kernel shells have also been employed in biodiesel production [15].

Active biochar obtained from pine waste has also proven effective in adsorbing cationic and anionic dyes, accompanied by a thorough analysis of its adsorption behavior and thermodynamic properties [16].

The efficacy of metal oxide-based materials and nanocomposites, such as CuO–Fe_2O_3 and rGO/Fe_3O_4/SnO_2, has been demonstrated in the removal of dye pollutants from aqueous solutions [17,18]. These findings highlight the urgent need to develop hydroxyapatite (HAp)/polyethylene glycol (PEG) composites based on conch shell waste as efficient and sustainable adsorbents for removing Rhodamine B from liquid waste. Thus, the objective of this study is to explore the synthesis and characterization of HAp/PEG 70:30 composites derived from natural gonggong shell precursors and to evaluate their potential as adsorbents for Rhodamine B (RhB) with superior performance, aiming to develop an environmentally friendly alternative in waste treatment technology. Thus, the objective of this study is to explore the synthesis and characterization of HAp/PEG 70:30 composites derived from natural gonggong shell precursors and to evaluate their potential as adsorbents for Rhodamine B (RhB) with superior performance, aiming to develop an environmentally friendly alternative in waste treatment technology.

Experimental

Materials

The material used in this study was gonggong clam shells (*Laevistrombus canarium*), which were obtained from a local market in Tanjungpinang, Riau Islands. Chemicals such as diammonium hydrogen phosphate ($(NH_4)_2HPO_4$), acetic acid (CH_3COOH 100%), ammonium hydroxide (NH_4OH 25%), sodium hydroxide (NaOH), and Rhodamine B were purchased from Merck. Additionally, phosphate and carbonate buffer solutions were used to regulate the pH, while deionized (DI) water was used as a solvent.

Methods

Preparation of calcined powder

The gonggong shell is cleaned with deionized water and dried at 105 °C for 24 hours. After drying, the shell is ground and calcined at 900 °C for 5 hours to produce calcium oxide (CaO). The chemical reaction during the calcination process is displayed in the following chemical reaction (1) [19].

$$CaCO_3 + \text{heat} \rightarrow CaO + CO_2 \quad (1)$$

Synthesis of HAp/PEG composite

HAp/PEG composites were synthesized with a composition ratio of 70:30 using the method detailed in the previous study [20]. Initially, 2 grams of CaO powder were weighed and dissolved in 71.4 mL of 1M CH_3COOH solution. The resulting solution was filtered, and dropwise additions of 118 mL of 0.18 M $(NH_4)_2HPO_4$

solution were made until a Ca/P molar ratio of 1.67 was achieved. Next, 1.536 grams of PEG were weighed and dissolved in 30 mL of deionized water before being gradually added to the mixture until it became homogeneous. The pH of the mixture was then adjusted to 11 using a 25% NH_4OH solution and stirred for 3 hours at 65 °C. Finally, the resulting HAp/PEG sol was filtered, dried at 110 °C for 5 hours, and the final product was labeled HAp/PEG.

Characterization

Characterization of HAp/PEG composites includes analysis of elemental composition, functional groups, crystallinity, specific surface area, and morphology. The composition of calcined gongong shell was analyzed using X-ray fluorescence spectroscopy (XRF, PANalytical Epsilon 3). Functional groups were analyzed using a Fourier Transform Infrared (FT-IR Spectrometer PerkinElmer) in the 4,000-500 cm^{-1} wavelength range. Crystallinity was tested with an X-Ray Diffractometer (XRD, PANanalytical X'Pert PRO-MPD PW3040/60) at an angle of 2θ = 10-90°, while crystal size was calculated using the Scherrer equation. The surface area was determined through the N_2 adsorption-desorption method using a Brunauer-Emmett-Teller (BET, Quantachrome NOVA 800) instrument. Morphological and elemental composition analysis was performed using Field Emission Scanning Electron Microscopy equipped with Energy Dispersive Spectroscopy (FESEM-EDS, Thermo Fisher Quattro S). In addition, the concentration of Rhodamine B before and after contact with the HAp/PEG composite was measured using a UV-Vis Spectrophotometer (Genesys 20 Thermo Scientific).

Determination of pH_{pzc}

The solid addition method determined the zero-charge point (pH_{pzc}). 0.1 g of HAp/PEG composite powder was added to 10 mL of 0.01 M NaCl solution. The solution's initial pH (pH_i) was adjusted using 0.1 M NaOH or HCl solution. The mixture was then stirred for 24 hours, centrifuged, and the final pH (pH_f) was measured. The pH_{pzc} value was obtained from the relationship between ΔpH and pH_i [21].

Batch adsorption studies

The HAp/PEG composite was tested for Rhodamine B adsorption by introducing 0.1 g of composite into 10 mL of dye solution with an initial concentration of 4 mg/L, at pH values ranging from 6 to 11. The pH of the solution was adjusted using 0.1 M NaOH or 0.1 M HCl, with buffer solution employed as a stabilizer. The influence of adsorbent dosage was examined at 0.05, 0.1, 0.15, 0.2, and 0.25 g, while the effect of contact time was studied at 30, 60, 90, 120, and 150 minutes under constant stirring at 250 rpm. Variations in initial dye concentration were investigated within the range of 4-100 mg/L. The residual RhB concentration in the filtrate was analyzed using a UV-Vis spectrophotometer at the maximum wavelength of 553 nm. The adsorption capacity of the composite was calculated using Equation (2), while the percentage of RhB removal was obtained by Equation (3). The adsorption mechanism was further evaluated through isotherm and kinetic studies, where equilibrium data were fitted to the Langmuir and the Freundlich models, and kinetic data were analyzed using the pseudo-first-order and pseudo-second-order models.

$$\text{Adsorption capacity } (q_e) = \frac{C_0 - C_e}{W} \times V \qquad (2)$$

$$\text{Percent removal of RhB } (\%R) = \frac{C_0 - C_e}{C_0} \times 100 \qquad (3)$$

Where, C_0 and C_e represent the initial and equilibrium concentrations of RhB (mg/L), respectively; V denotes the volume of the solution (L); W is the mass of the adsorbent (g); q_e represents the adsorption capacity (mg/g); and %R indicates the percentage of RhB removal.

Reusability study

The HAp/PEG composite regeneration after Rhodamine B adsorption was carried out using a 0.1 M NaOH eluent. 0.15 g of the composite was introduced into 10 mL of a 20 mg/L RhB solution at pH 11, adjusted with buffer, and stirred for 120 minutes at 250 rpm under room temperature conditions. The produced precipitate was centrifuged and dried. Subsequently, the dried precipitate was immersed in 10 mL of 0.1 M NaOH solution and treated under the same conditions as the adsorption process to release the bound RhB. Following desorption, the precipitate was washed with distilled water until neutrality was achieved, and then dried again for use in the subsequent regeneration cycle. This adsorption-desorption process was repeated multiple times to evaluate the stability and reusability of the HAp/PEG composite.

Results and Discussion

Elemental composition

The elemental composition study of a calcined gonggong shell is shown in Table 1. Calcined gonggong shell powder has calcium as the dominant, followed by silica (Si), aluminum (Al), and phosphorus (P). The high calcium concentration supports the appropriateness of gonggong shell as a natural precursor for the synthesis of hydroxyapatite, which is consistent with earlier studies on bamboo shells, which also found calcium to be its main component [22].

Table 1. The X-ray fluorescence of Gonggong shell

Compounds	Composition (%)
CaO	95.089
P_2O_5	1.014
Al_2O_3	0.447
SiO_2	0.163
Others	3.287

Vibrational results

The FTIR spectrum of the HAp/PEG composite is shown in Figure 1, confirming the presence of characteristic functional groups from both components. The broad absorption band at 3,433 cm^{-1} indicates the stretching vibration of the -OH group originating from HAp and PEG. The phosphate group (PO_4^{3-}) is marked by sharp peaks at 564 cm^{-1} (bending vibration), 602 cm^{-1} (symmetric stretching), and 1,036 cm^{-1} (symmetric stretching) [19]. Additionally, the characteristic band of PEG is detected at 1,455 cm^{-1} associated with the C-H group. The absence of clear absorption bands from the C=O and C–O groups in this spectrum is likely due to the low concentration of PEG and overlap with the phosphate band of HAp, indicating a strong interaction between PEG and HAp [23]. This is reinforced by the report from Azzaoui *et al.* (2023), which states that the dissolution of PEG in water produces PEG-OH, which is capable of coordinating with Ca^{2+} and PO_4^{3-} ions, thereby supporting the formation of a stable HAp/PEG composite structure [11].

Crystallographic result

Figure 2 presents the XRD spectrum of the HAp/PEG composite. The diffraction pattern reveals sharp peaks, indicating a high HAp crystallinity degree. The characteristic positions are observed at 2θ values of 25.92°, 29.40°, 31.74°, 32.25°, 34.08°, 39.40°, 46.72°, 49.51°, and

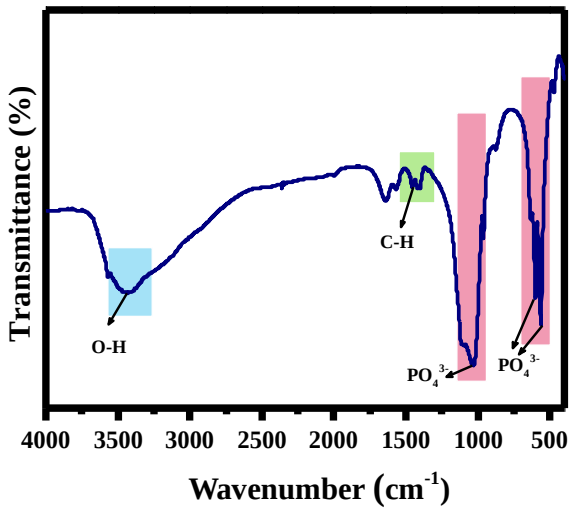

Figure 1. FT-IR spectrum of HAp/PEG composite

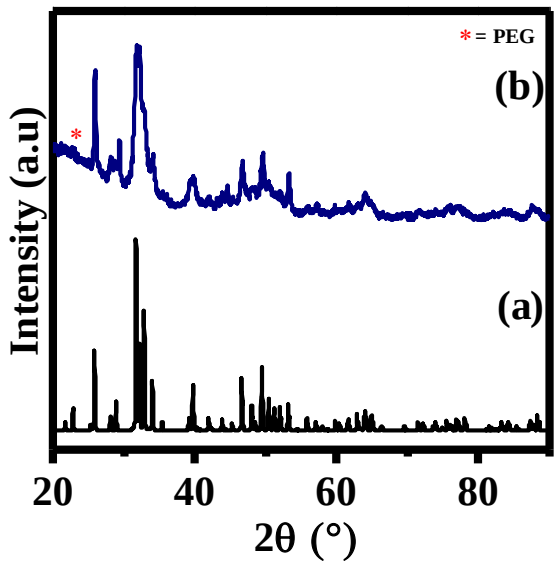

Figure 2. XRD patterns of (a) standard Hap and (b) HAp/PEG composite

53.29°, which correspond to the ICSD standard #157481.

These results confirm that HAp is formed in a hexagonal structure with an average crystallite size of 31.64 nm, as calculated using the Scherrer equation. Additionally, a weak peak at 23.2° indicates the presence of PEG, but it does not interfere with the HAp crystal structure [8]. PEG regulates HAp crystal growth by inhibiting the release of Ca^{2+} ions and slowing crystal nucleation, resulting in relatively larger crystallite sizes [24]. This finding is consistent with other reports suggesting that compositing HAp with polymers, such as alginate, also modifies crystallite size, with pure HAp having a smaller size than composite HAp [22].

The high crystallinity and phase purity achieved significantly contribute to structural stability and the availability of active sites, which are crucial for practical adsorption applications [25].

Morphology results

Figure 3 shows FESEM images of HAp/PEG composites, revealing irregular morphology with particle sizes varying from small to large (Figure 3a). Further magnification reveals a fine pore network formed due to the interaction of PEG with HAp, where PEG molecules surround Ca^{2+} ions, thereby reducing the tendency for crystal agglomeration and resulting in a better pore distribution [23]. These delicate pores are important for increasing the specific surface area and enlarging the capacity to trap pollutant molecules, thereby strengthening the potential for adsorption applications [26].

EDS analysis (Figure 3b) shows the main elements that make up hydroxyapatite (Ca, P, and O) and the C element from PEG. The Ca/P ratio of the composite was obtained as 1.85, which is higher than the stoichiometric ratio of pure HAp (1.67), indicating the success of HAp compositing with PEG [8].

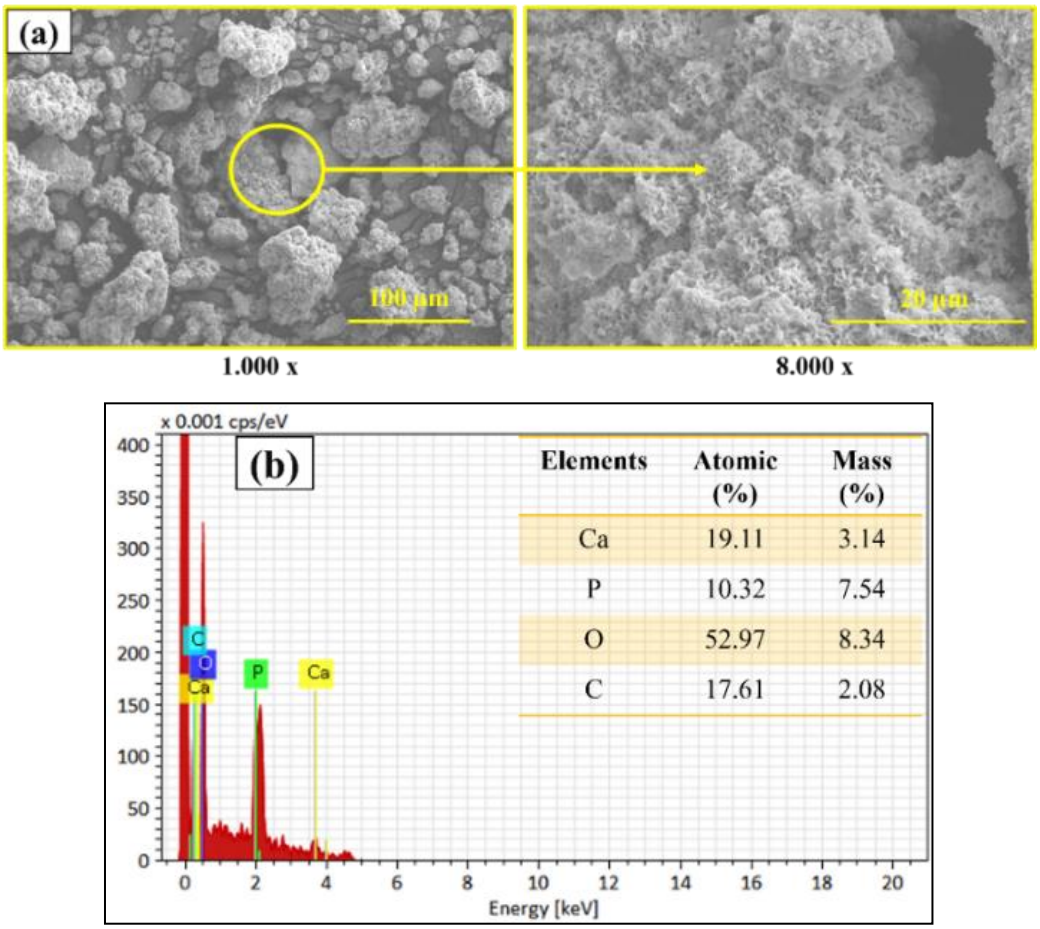

Figure 3. (a) SEM images of the HAp/PEG 70:30 composite observed at magnifications of 1,000 (left) and 8,000 (right), (b) EDS spectrum of the HAp/PEG composite

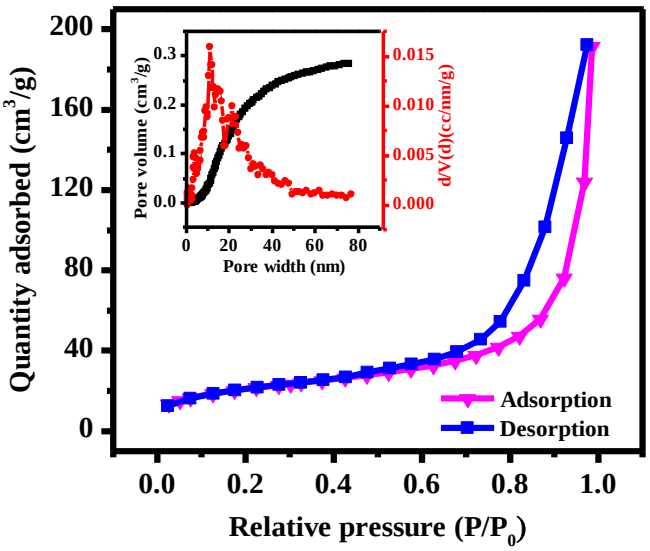

Figure 4. BET specific surface area (pore size distribution and pore volume inset) measured from N_2 adsorption-desorption isotherms on HAp/PEG composites

BET analysis

Figure 4 shows the results of the BET analysis of the HAp/PEG composite with a specific surface area of 73.001 m^2/g, pore volume of 0.285 cm^3/g, and average pore size of 12.11 nm. The nitrogen adsorption-desorption isotherm follows type IV, indicating mesoporous characteristics. The surface area value is relatively large compared to previous reports [24]. A large surface area provides significant advantages, as it can increase the adsorption capacity of materials toward pollutants [27].

Batch mode adsorption studies

Determination of pH_{pzc}

pH_{pzc} is an important parameter in understanding the properties of adsorbent surfaces because it determines the interaction between the material surface and the adsorbate molecules. An adsorbent surface with a balance of positive and negative charges (zero charge point) is shown in Figure 5. Based on the results

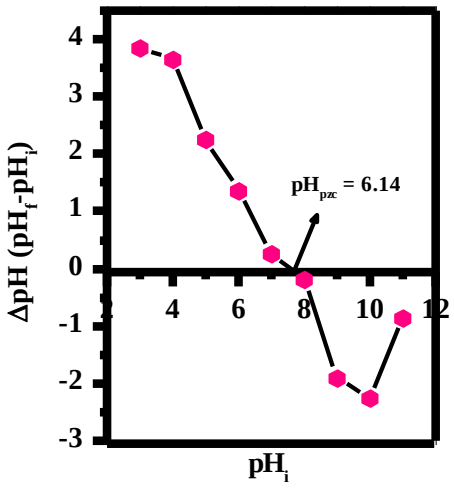

Figure 5. Point of zero charge of HAp/PEG composite

of the ΔpH curve against pH_i, the pH_{pzc} value of the HAp/PEG composite was obtained to be 6.14. When the pH of the solution is higher than the pH_{pzc} value, the adsorbent surface is negatively charged, while at pH conditions lower than pH_{pzc}, the surface tends to be positively charged [28].

This explains that cationic RhB dye interacts more easily with the surface of the HAp/PEG composite at pH conditions above pH_{pzc}, thereby increasing the adsorption capacity. In contrast, at pH conditions below 6.14, the positive charge on the adsorbent surface is not favorable for the adsorption of anionic molecules [21,29].

Effect of pH

The pH of the solution plays an important role in the dye removal process [30]. Based on the pHpzc determination results, the HAp/PEG composite was more effective at absorbing Rhodamine B (RhB) at a pH above 6.14. Figure 6 shows that the efficiency of RhB removal increased with an increase in solution pH, with an optimum value achieved at pH 11 of 88.08% and an adsorption capacity of 0.3523 mg/g. These optimal conditions were obtained using 10 mL of RhB solution with a concentration of 4 ppm, 0.1 g of HAp/PEG composite mass, a stirring speed of 250 rpm, and a contact time of 60 minutes. The increase in removal percentage was in line with the increase in adsorption capacity, as reported in previous studies [31,32]. However, at pH above 11, spontaneous decolorization occurred due to RhB degradation before adding the adsorbent. The dominant interaction mechanism is the electrostatic force between the negatively charged active sites on the surface of the HAp/PEG composite and the positively charged RhB molecules [33].

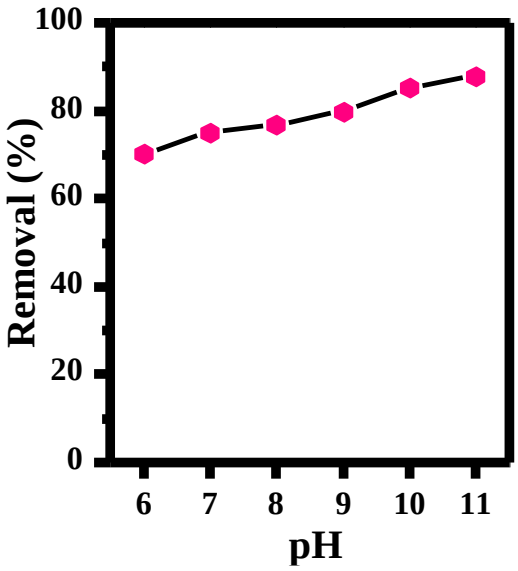

Figure 6. Effect of pH on RhB dye adsorption

Effect of adsorben dosage

The adsorbent dose is important for providing an adequate number of active sites and surface area for adsorption [34]. The variation in the dosage of HAp/PEG composite for the removal of Rhodamine B (RhB) was studied in the range of 0.05–0.25 g with fixed parameters of RhB concentration at 4 mg/L, pH 11, solution volume of 10 mL, contact time of 60 minutes, and stirring speed of 250 rpm.

The results showed that the optimum dose was achieved at 0.15 g with a removal percentage of 91.25% and an adsorption capacity of 0.2433 mg/g (Figure 7). Increasing the adsorbent dose to the optimum point increased the number of active sites, thereby enhancing the chance of interaction between RhB and the composite surface [35]. However, adding doses above 0.15 g reduced adsorption capacity due to particle agglomeration and overlap between active sites [36]. These findings confirm that selecting the optimal dose is crucial for obtaining the maximum adsorption performance while maintaining material usage efficiency.

Effect of RhB dye concentration

The initial concentration of the dye is an important factor in evaluating the maximum capacity of the adsorbent to absorb dye molecules [37]. Variations in RhB concentration were studied in the range of 4–100 mg/L with other conditions held constant.

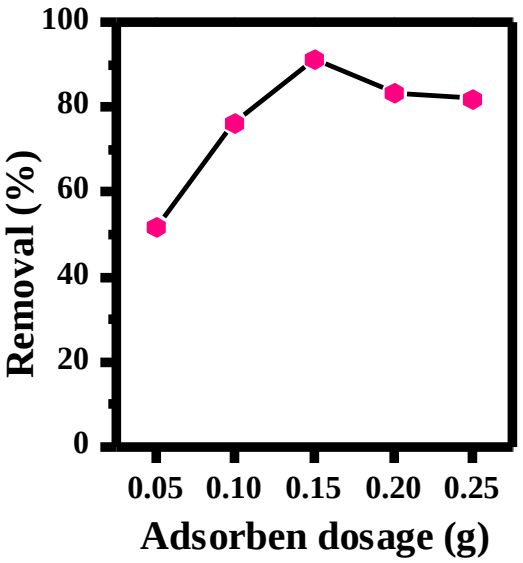

Figure 7. Effect of adsorben dosage on RhB dye adsorption

The results showed that the optimum concentration was achieved at 20 mg/L with a removal rate of 92.94% and an adsorption capacity of 1.2391 mg/g (Figure 8). RhB molecules can be adsorbed at low concentrations efficiently because the number of available active sites on the HAp/PEG composite is still sufficient. Conversely, at high concentrations, RhB molecules compete to occupy adsorption sites, resulting in saturation and decreased removal efficiency [38].

Effect of contact time

Contact time is an important parameter in determining the equilibrium of the adsorption process between the adsorbent and the adsorbate molecule [32]. A contact time variation of 30-120 minutes was used to examine the performance of the HAp/PEG composite in absorbing RhB, with other conditions remaining constant. The adsorption capacity increased with time, reaching an optimum condition at 120 minutes with a capacity of 1.2423 mg/g and a removal rate of 93.17% (Figure 9).

The significant increase in the early minutes was due to the abundance of active sites. However, after 120 minutes, the adsorption rate decreased, indicating that most active sites were saturated and the system was approaching equilibrium [2]. These findings confirm that contact time is important in ensuring adsorption effectiveness and material composite efficiency [39].

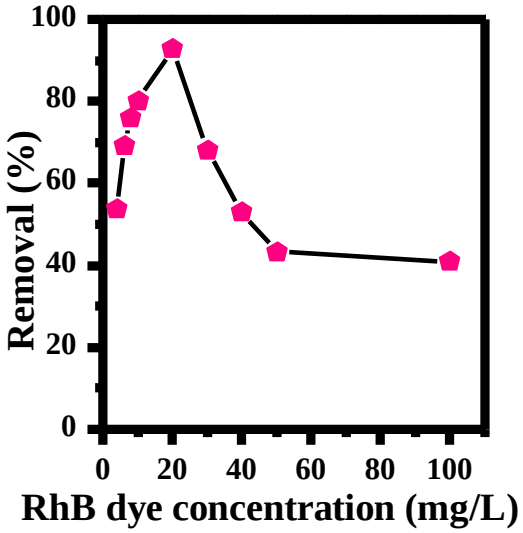

Figure 8. Effect of the initial concentration of RhB dye on adsorption by HAp/PEG composite

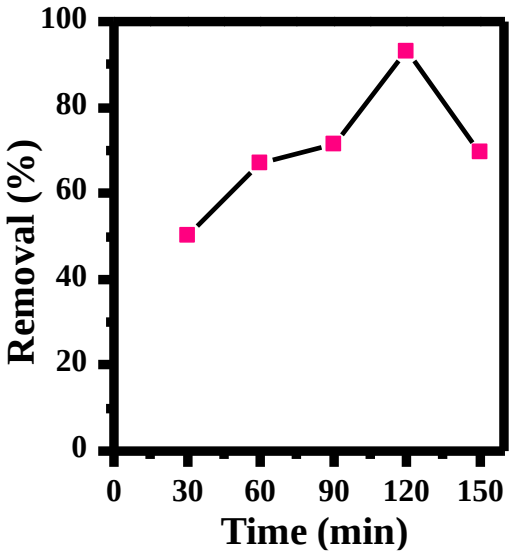

Figure 9. Effect contact time on RhB dye adsorption

Adsorption Isotherm

Adsorption isotherm studies provide information about the interaction between the adsorbent and the adsorbate. Based on data on the effect of initial RhB concentration variation, the type of isotherm can be plotted and analyzed. The experimental data were evaluated using two commonly used adsorption isotherm models, the Langmuir and the Freundlich models. According to the Langmuir model, adsorption between adsorbent and adsorbate occurs at a homogeneous site with the formation of a monolayer, as stated in Equation 4 [40]:

$$\frac{C_e}{q_e} = \frac{1}{K_l q_m} + \frac{C_e}{q_m} \quad (4)$$

According to the Freundlich model, adsorption takes place on heterogeneous surfaces and is reversible, resulting in the formation of multilayer layers, as expressed in Equation 5:

$$\log q_e = \log K_f + \frac{1}{n} \log C_e \quad (5)$$

In the presented model, K_F (mg/g) is the Freundlich constant and 1/n indicates the surface heterogeneity factor. All constants and correlation coefficients obtained from the two isotherm models are summarized in Figure 10 and Table 2. The analysis results show that the Langmuir isotherm has a higher R^2 value than the Freundlich isotherm. This indicates that the adsorption process of RhB by the HAp/PEG composite tends to follow the Langmuir model, which occurs in a monolayer. This mechanism occurs through the interaction of the -OH group on the surface of the HAp/PEG composite with the cationic part of the RhB molecule [41]. Additionally, the equilibrium factor (R_L) analysis results show that the adsorption process is favorable, with an R_L value of 0.821. Similar studies have been reported for the adsorption isotherm of RhB dye on various adsorbents that follow the Langmuir isotherm model [32,42,43].

Adsorption Kinetics

Adsorption kinetics aims to identify a suitable model for characterizing the adsorption process, so that it can be determined whether the interaction between the adsorbent and adsorbate occurs through a chemical mechanism (chemisorption) or a physical mechanism (physisorption) (Rich *et al.*, 2021). Kinetic data were obtained from experiments with varying contact times and analyzed using two models, namely the first-order pseudo model and the second-order pseudo model.

The first-order pseudo model is expressed in Equation 6 [40]:

$$\ln (q_e - q_t) = \ln q_e - k_1 t \quad (6)$$

Where, k_1 (min^{-1}) is the pseudo-first-order rate constant, q_e (mg/g) and q_t (mg/g) are the adsorption capacities at equilibrium and at each time t (min), respectively.

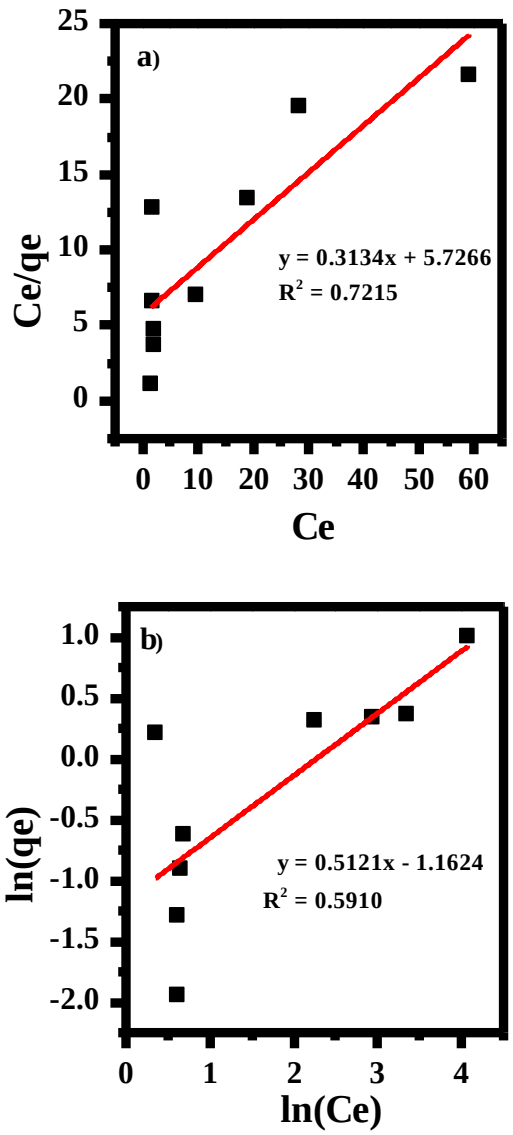

Figure 10. Langmuir isotherm (a) Freundlich isotherm for adsorption of RhB dye

Table 2. Langmuir and Freundlich parameters for adsorption of RhB onto HAp/PEG composite

Langmuir				Freundlich		
q_m (mg/g)	K_L (L/mg)	R_L	R^2	K_F (mg/g)	n	R^2
3.19	0.0547	0.821	0.7215	0.0688	1.952	0.5910

Additionally, the pseudo second-order model is expressed in Equation 7:

$$\frac{t}{q_t} = \frac{1}{k_2 q_e^2} + \frac{1}{q_e} t \quad (7)$$

Where, k_2 (g/mg.min) is the pseudo-second-order rate constant.

Based on Figure 11 and Table 3, the second-order pseudo model shows a higher R^2 value than the first-order pseudo model. This result indicates that the adsorption mechanism is controlled by chemisorption, where electrostatic interactions occur between charged groups on the surface of the HAp/PEG composite and RhB molecules. The calculated qe value (q_e, cal) is in line with the experimental value (qe,exp), thereby reinforcing the suitability of the pseudo-second-order model for the experimental data. This finding is consistent with previous reports on RhB adsorption on various adsorbents that follow the pseudo-second-order model [12,30,32].

The regeneration process of HAp/PEG composites is an important aspect for evaluating their long-term usability. This study tested HAp/PEG composites through several adsorption-desorption cycles. The desorption process was performed by contacting the composites with 10 mL of NaOH solution (0.1 M) for 120 minutes. NaOH was chosen as the eluent based on its basic properties, which can break the bonds between the HAp/PEG composite and RhB molecules, allowing the dye molecules to be released again [44]. The reuse performance of the HAp/PEG composite is shown in Figure 12. The results indicate that the composite remains efficient in removing RhB after four regeneration cycles, with removal percentages of 96.08%,

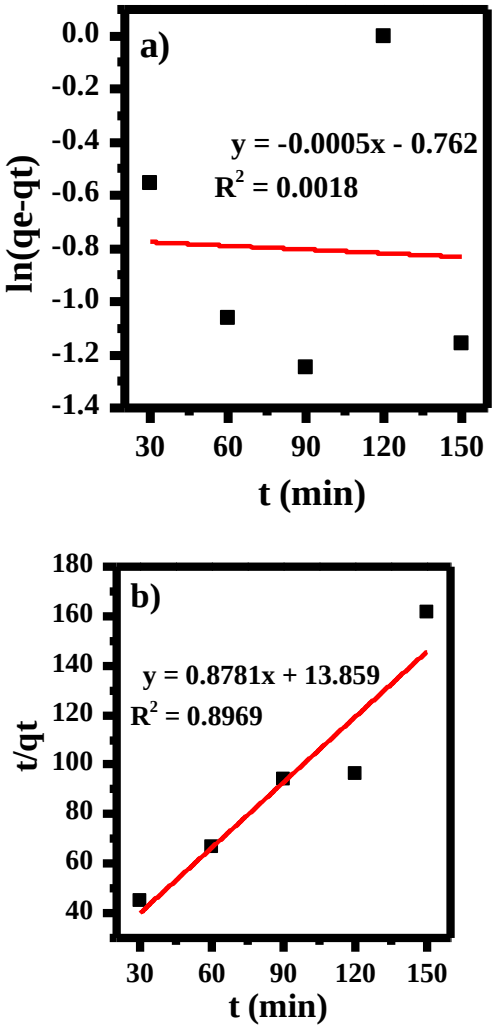

Figure 11. Pseudo-first order kinetics (a) Pseudo-second order kinetics and (b) of HAp/PEG composite

Table 3. Kinetic data predicted by pseudo-first order and pseudo second order kinetic models for the adsorption of RhB onto HAp/PEG composite

Pseudo-Frist Order				Pseudo-Second Order		
q_e.exp (mg/g)	q_e,cal (mg/g)	k_1 (min^{-1})	R^2	q_e,cal (mg/g)	k_2 (min^{-1})	R^2
1.2400	0.4670	0.0004	0.0018	1.139	0.0556	0.8969

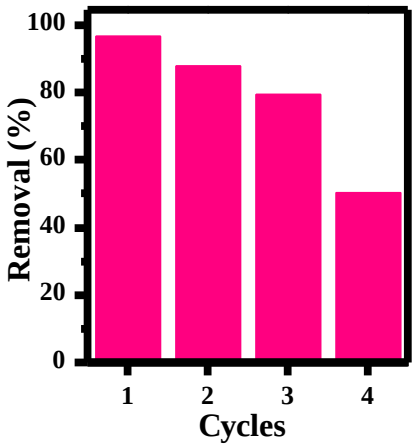

Figure 12. The removal efficiency of RhB dye by the HAp/PEG composite at different regeneration cycles

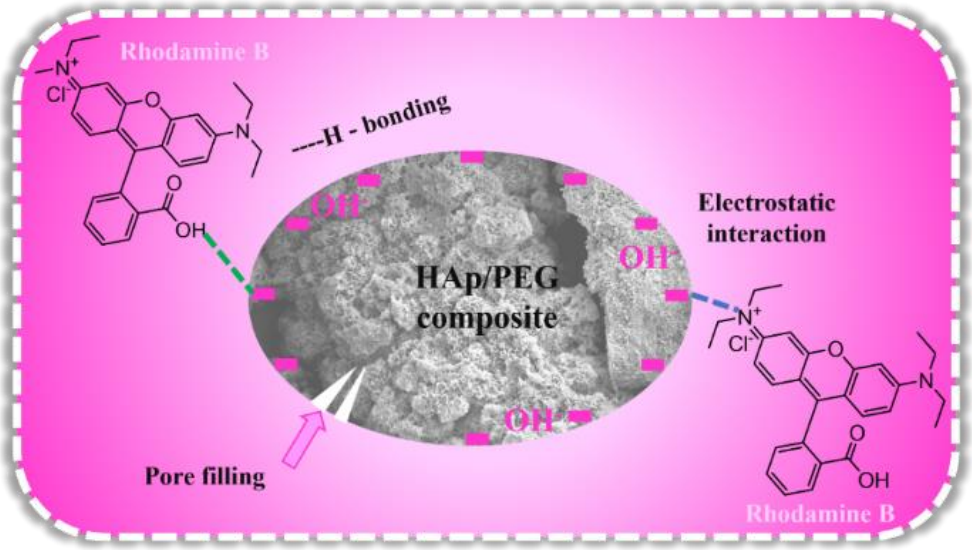

Figure 13. Possible mechanism of RhB adsorption onto HAp/PEG composite

88.03%, 79.52%, and 50.75%, respectively. These findings demonstrate that the HAp/PEG *Regeneration* composite has good regeneration capabilities and holds the potential to be an effective adsorbent material for repeated applications in the removal of organic pollutants from aquatic environments.

Adsorption mechanism

Based on the HAp/PEG composite characterization results and its application in the adsorption process of RhB dye, the possible adsorption mechanism can be explained as follows. As illustrated in Figure 13, FTIR characterization shows that HAp/PEG composites are rich in -OH, PO_4^{3-}, and C-H functional groups that facilitate bonding with RhB molecules. XRD results confirm the crystallinity of HAp/PEG composites, which potentially supports bonding with RhB molecules. Additionally, the high specific surface area and smooth particle morphology increase

the contact between the composite and RhB molecules, thereby enhancing adsorption interactions. The RhB structure has positively charged N^+ groups that can interact with negatively charged sites on the adsorbent surface. Isotherm and adsorption kinetics analyses support this mechanism, showing the formation of a monolayer and a tendency for chemisorption interactions. Therefore, the mechanism of RhB adsorption by the HAp/PEG composite can involve electrostatic interactions, hydrogen bonding, and adsorption through pore filling.

Conclusion

This study demonstrates that gonggong shell waste (*Laevistrombus canarium*) has the potential to serve as a natural source of calcium precursors for the synthesis of hydroxyapatite/polyethylene glycol (HAp/PEG) composites using the in-situ sol-gel method. The resulting composite exhibits characteristic functional groups and crystallinity that meets the standards of ICSD#157481, along with an irregular spherical morphology and a high specific surface area. In adsorbing Rhodamine B (RhB) dye, optimal conditions were identified at pH 11, an adsorbent mass of 0.15 g, an initial concentration of 20 mg/L, and a contact time of 120 minutes. The adsorption process adheres to the Langmuir isotherm model, indicating monolayer formation, and follows pseudo-second-order kinetics. The main adsorption mechanisms include hydrogen bonding, electrostatic interactions, and pore filling. Additionally, the HAp/PEG composite displayed the ability to regenerate up to four cycles without significant performance loss. These findings confirm that the HAp/PEG composite derived from gonggong shell waste is a sustainable and environmentally friendly adsorbent material, with potential applications in wastewater treatment and environmental remediation.

Acknowledgements

This research was funded by the Directorate of Research and Community Service, Directorate General of Research and Development, Ministry of Education, Science, and Technology under the Fundamental Research Scheme – Regular, in accordance with Research Contract Number: 060/C3/DT.05.00/PL/2025, Fiscal Year 2025.

Authors' Contributions

All authors contributed to data analysis, drafting, and revising of the paper and agreed to be responsible for all the aspects of this work.

ORCID

Novesar Jamarun
https://orcid.org/0000-0001-8284-145X
Zulhadjri
https://orcid.org/0000-0003-1406-3443
Upita Septiani
https://orcid.org/0000-0002-1846-3105
Vivi Sisca
https://orcid.org/0000-0001-9325-5990
Arika Prasejati
https://orcid.org/0009-0000-0566-2909
Cynthia
https://orcid.org/0009-0004-8677-7423
Nabiila Ayyu Trycahyani
https://orcid.org/0009-0009-1189-0954
Adam Hidayat
https://orcid.org/0009-0001-0904-7169

References

[1] Wang, C., Ahmad, S.F., Ayassrah, A.Y.B.A., Awwad, E.M., Irshad, M., Ali, Y.A., Al-Razgan, M., Khan, Y., Han, H. An empirical evaluation of technology acceptance model for artificial intelligence in e-commerce. *Heliyon*, **2023**, 9(8).

[2] Jiao, C., Liu, D., Wei, N., Gao, J., Fu, F., Liu, T., Wang, J. Efficient congo red removal using porous cellulose/gelatin/sepiolite gel beads: Assembly, characterization, and adsorption mechanism, *Polymers*, **2021**, 13 (22), 3890.

[3] Ali, F., Zahid, S., Khan, S., Ur, R.S., Ahmad, F. A comprehensive review on adsorption of dyes from aqueous solution by mxenes. *Asian Journal of Green Chemistry*, **2024**, 8, 81.

[4] Pervez, M. N., Jahid, M. A., Mishu, M. M. R., Talukder, M. E., Buonerba, A., Jiang, T., Liang, Y., Tang, S., Zhao, Y., Dotto, G. L., Cai, Y., Naddeo, V. Tuning the surface functionality of polyethylene glycol-modified graphene oxide/chitosan composite for efficient removal of dye. *Scientific Reports*, **2023**, 13 (1), 13460.

[5] Jamarun, N., Gihwani, G., Septiani, U., Yadris, F., Refki Novesar, M., Rahmadani Putri, D. Synthesis and characterization of hydroxyapatite composite of cuttlefish bone (Sepia Sp.) with gelatin as Rhodamine b dye adsorbent. *ChemistrySelect*, **2024**, 9 (40), e202403095.

[6] Ayoub, H.A., Khairy, M., Rashwan, F.A., Abdel, H.H.F. Synthesis of calcium silicate hydrate from chicken eggshells and combined joint effect with nervous system insecticides. *Asian Journal of Green Chemistry*, **2022,** 6, 103.

[7] Xu, J., Mucalo, M. R., Pickering, K. L. Bioinspired surface modification of mussel shells and their application as a biogenic filler in polypropylene composites. *Composites Part C: Open Access*, **2024**, 15, 100520.

[8] Jamarun, N., Amelia, D., Septiani, U., Sisca, V. The effect of temperature on the synthesis and characterization of hydroxyapatite-polyethylene glycol composites by in-situ process. *Hybrid Advances*, **2023**, 2, 100031.

[9] Anitta, S., Sekar, C. Voltammetric determination of paracetamol and ciprofloxacin in the presence of vitamin C using cuttlefish bone-derived hydroxyapatite sub-microparticles as electrode material. *Results in Chemistry*, **2023**, 5, 100816.

[10] Subramanian, R., Sathish, S., Murugan, P., Mohamed Musthafa, A., Elango, M. Effect of piperine on size, shape and morphology of hydroxyapatite nanoparticles synthesized by the chemical precipitation method. *Journal of King Saud University - Science*, **2019**, 31 (4), 667–673.

[11] Azzaoui, K., Aaddouz, M., Akartasse, N., Mejdoubi, E., Jodeh, S., Hammouti, B., Taleb, M., Es-Sehli, S., Berisha, A., Rhazi, L. Synthesis of β-tricalcium phosphate/peg 6000 composite by novel dissolution/precipitation method: Optimization of the adsorption process using a factorial design—dft and molecular dynamic. *Arabian Journal for Science and Engineering*, **2024**, 49(1), 711-732.

[12] Jamarun, N., Prasejati, A., Zulhadjri, Z., Caniago, S., Amirullah, T. Y., Wulandari, W., Sisca, V. Effect of chitosan concentration on hydroxyapatite/chitosan composite synthesis using the in-situ method as a dye adsorbent. *Kuwait Journal of Science*, **2024**, 51 (4), 100252.

[13] Jamarun, N., Trycahyani, N.A., Arief, S., Septiani, U., Sisca, V. Synthesis of hydroxyapatite-polyethylene glycol with in-situ method using calcium oxide from blood shells (anadara granosa). *Indonesian Journal of Chemistry*, **2023**, 23(3), 618-626.

[14] Daefisal, O.L., Yanti, D.D., Reagen, M.A., Yudha, S.S., Hendri, J. Hydrothermal carbonization of coconut pulp and the adsorption activity toward methylene blue. *Advanced Journal of Chemistry, Section A*, **2024**, 7, 386**.**

[15] Odeh, L. U., Nnanyelugo, C. E., Adams, A., Abubakar, S. A., Ejikeme, C. S., Igwe, E. P., Ibeanu, U. E., Eze, S. O., Okpako, O., Ogamba, C., Ekhafe, M. O., Abah, V. E., Nwafor, C., H., Zakari, A. The synthesis and characterization of biobased catalyst derived from palm kernel shell and eggshell for the production of biodiesel. *Advanced Journal of Chemistry, Section B: Natural Products and Medical Chemistry*, **2024**, 6(4), 405-422.

[16] Aljeboree, A.M., Hadi, E.S., Alalaq, I.S., Hussein, T.K., Altimari, U.S., Alkaim, A.F. Efficient removal of cationic and anionic dyes using hcl-activated biochar from pine waste: Adsorption behavior and thermodynamic insights. *Advanced Journal of Chemistry Section A*, **2025**, 8, 1233-1246.

[17] Einad, N.A., Merza, M.M., Ismail, A.H. Experimental and DFT studies of comparison between CuO and CuO-Fe_2O_3 to remove dye pollutants from aqueous solution. *Advanced Journal of Chemistry, Section A*, **2025**, 8 (4), 700-715.

[18] Ismail, A.F., Al-Abodi, E.E. Synthesis and characterization of rGo/Fe_3O_4/SnO_2 nanocomposite to remove terasil black dye from aqueous solutions. *Advanced Journal of Chemistry, Section A*, **2025**, 8, 687.
[19] Jamarun, N., Ummairah, D. U., Putri, Y. E., Septiani, U., Amirullah, T. Y. Cuttlefish (Sepia Sp.) derived heat resistance hydroxyapatite/alginate composites through the sol-gel method. *Rasayan Journal of Chemistry*, **2024**, 17 (2), 598–604.
[20] Jamarun, N., Caniago, S., Septiani, U., Prasejati, A., Wulandari, W., Amirullah, T. Y. Synthesis and characterization of hydroxyapatite composite from cuttlebone (Sepia Sp.) with chitosan via in situ as antibacterial. *ChemistrySelect*, **2024**, 9 (3), e202303514.
[21] Bourachdi, S. El; El Ouadrhiri, F., Moussaoui, F., Saleh, E. A. M., Amri, A. El, Althomali, R. H., Kassem, A. F., Moharam, M. M., Ayub, A. R., Husain, K., Hassan, I., Lahkimi, A. Enhancing graphene oxide production and its efficacy in adsorbing crystal violet: An in-depth study of thermodynamics, kinetics, and DFT analysis. *International Journal of Chemical Engineering*, **2024**, 2024, 1-25.
[22] Wulandari, W., Islami, D.M., Wellia, D.V., Emriadi, E., Sisca, V., Jamarun, N. The effect of alginate concentration on crystallinity, morphology, and thermal stability properties of hydroxyapatite/alginate composite. *Polymers*, **2023**, 15(3), 614.
[23] Jegatheeswaran, S., Sundrarajan, M. PEGylation of novel hydroxyapatite/peg/ag nanocomposite particles to improve its antibacterial efficacy. *Materials Science and Engineering: C*, **2015**, 51, 174-181.
[24] Azzaoui, K., Jodeh, S., Mejdoubi, E., Hammouti, B., Taleb, M., Ennabety, G., Berisha, A., Aaddouz, M., Youssouf, M., Shityakov, S. Synthesis of hydroxyapatite/polyethylene glycol 6000 composites by novel dissolution/precipitation method: Optimization of the adsorption process using a factorial design: Dft and molecular dynamic. *BMC Chemistry*, **2023**, 17(1), 150.
[25] Hariani, P. L., Said, M., Rachmat, A., Sari, S. P. Hydroxyapatite-Peg/Fe_3O_4 Composite for adsorption of phenol from aqueous solution. *Polish Journal of Environmental Studies*, **2021**, 30 (2), 1621–1629.
[26] Azzaoui, K., Mejdoubi, E., Lamhamdi, A., Lakrat, M., Hamed, O., Jodeh, S., Berrabah, M., Elidrissi, A., El Meskini, I., Daoudi, M. Preparation of hydroxyapatite biobased microcomposite film for selective removal of toxic dyes from wastewater. *Desalination and Water Treatment*, **2019**, 149, 194-208.
[27] Peighambardoust, S.J., Vatankhah, M., Pakdel, P.M., Foroutan, R., Mohammadi, R. Carboxymethyl cellulose/activated carbon/hydroxyapatite composite adsorbent for remediation of methylene blue from water media. *International Journal of Biological Macromolecules*, **2024**, 276, 133764.
[28] Correa, P.A.P., Buenaventura, S.F.O., Santos, J.R.S., Lopez, E.C.R. Optimization of chitosan/polyvinyl alcohol/lemongrass hydrochar composite beads for the removal of azo dyes in water. *Next Materials*, **2025**, 8, 100621.
[29] Alhogbi, B. G., Altayeb, S., Bahaidarah, E. A., Zawrah, M. F. Removal of anionic and cationic dyes from wastewater using activated carbon from palm tree fiber waste. *Processes*, **2021**, 9 (3), 416.
[30] Alam, S., Ullah, R., ur Rahman, N., Ilyas, M., Ullah, S., Zahoor, M., Umar, M. N., Ullah, R., Ali, E. A. Synthesis of metallic nanoparticles and its application in adsorption of Metanil yellow and Rhodamine B from aqueous solutions. *Desalination and Water Treatment*, **2023**, 313, 186–195.
[31] Cui, L., Wang, Y., Hu, L., Gao, L., Du, B., Wei, Q. Mechanism of pb (ii) and methylene blue adsorption onto magnetic carbonate hydroxyapatite/graphene oxide. *RSC Advances*, **2015**, 5(13), 9759-9770.
[32] Jinendra, U., Bilehal, D., Nagabhushana, B., Kumar, A.P. Adsorptive removal of rhodamine b dye from aqueous solution by using graphene–based nickel nanocomposite. *Heliyon*, **2021**, 7(4).
[33] Zhai, Q.Z. Adsorption of rhodamine b dye on potassium permanganate modified peanut shell: Adsorption kinetics, thermodynamics and isotherm studies. *Desalination and Water Treatment*, **2023**, 303, 212-223.
[34] Errich, A., Azzaoui, K., Mejdoubi, E., Hammouti, B., Abidi, N., Akartasse, N., Benidire, L., Hajjaji, S.E., Sabbahi, R., Lamhamdi, A. Toxic heavy metals removal using a hydroxyapatite and hydroxyethyl cellulose modified with a new Gum Arabi. *Indonesian Journal of Science and Technology*, **2021**, 6(1), 41-64.

[35] Chahkandi, M. Mechanism of congo red adsorption on new sol-gel-derived hydroxyapatite nano-particle. *Materials Chemistry and Physics*, **2017**, 202, 340-351.

[36] Nyakairu, G.W.A., Kapanga, P.M., Ntale, M., Lusamba, S.N., Tshimanga, R.M., Ammari, A., Shehu, Z. Synthesis, characterization and application of Zeolite/Bi_2O_3 nanocomposite in removal of rhodamine b dye from wastewater. *Cleaner Water*, **2024**, 1, 100004.

[37] Husain, A., Ansari, K., Mahajan, D.K., Kandasamy, M., Ansari, M., Giri, J., Al-Lohedan, H.A. Harnessing sustainable n-doped activated carbon from walnut shells for advanced all-solid-state supercapacitors and targeted rhodamine b dye adsorption. *Journal of Science: Advanced Materials and Devices*, **2024**, 9(2), 100699.

[38] Kjidaa, B., Mchich, Z., Saffaj, T., Saffaj, N., Mamouni, R. Harnessing fish scales: Bio-hydroxyapatite and novel bio-hydroxyapatite@ polypyrrole nanocomposite for advanced oxytetracycline antibiotic adsorption. *Journal of Water Process Engineering*, **2024**, 68, 106515.

[39] Chouchane, T., Abedghars, M. T., Chouchane, S., Boukari, A. Improvement of the sorption capacity of methylene blue dye using slag, a steel by product. *Kuwait Journal of Science*, **2024**, 51(2), 100210**.**

[40] Jebli, A.; Amri, A. El; Hsissou, R.; Lebkiri, A.; Zarrik, B.; Bouhassane, F. Z.; Hbaiz, E. mahdi; Rifi, E. H.; Lebkiri, A. Synthesis of a chitosan@hydroxyapatite composite hybrid using a new approach for high-performance removal of crystal violet dye in aqueous solution, equilibrium isotherms and process optimization. *Journal of the Taiwan Institute of Chemical Engineers*, **2023**, 149, 105006.

[41] Ouardi, Y. El, Aissouq, A. El, Chennah, A., Ouammou, A., Laatikainen, K. Synthesis, characterization, and DFT investigation of Rhodamine B dye removal by activated carbon produced from Argan nutshell. *Biomass Conversion and Biorefinery*, **2024**, 14 (13), 15107–15118.

[42] Liu, Z., Huang, X., Miao, Y., Gao, B., Shi, Y., Zhao, J., Tan, S.H. Eggplant biomass based porous carbon for fast and efficient dye adsorption from wastewater. *Industrial Crops and Products*, **2022**, 187, 115510.

[43] Chang, S., Zhang, X., Wang, C., Bai, J., Li, X., Liang, W., Mao, Y., Cai, J., Li, Y., Jiang, Y. Efficient adsorption of rhodamine b using synthesized mgal hydrotalcite/sodium carboxymethylcellulose/sodium alginate hydrogel spheres: Performance and mechanistic analysis. *Heliyon*, **2024**, 10(9).

[44] Venkatesan, A., Srividhya, B., Alajmi, A., Sadeq, A. M., Chava, R. K., Habila, M. A., Senthil Kumar, D., Guganathan, L., Ragupathy, S. High adsorption capacities of Rhodamine B dye by activated carbon synthesized from cotton stalks agricultural waste by chemical activation. *Ceramics International*, **2025**, 51 (10), 13345–13354.

HOW TO CITE THIS MANUSCRIPT

N. Jamarun, Zulhadjri, U. Septiani, V. Sisca, A. Prasejati, Cynthia, N.A. Trycahyani, A. Hidayat. Eco-Friendly Waste-to-Resource Synthesis of Hydroxyapatite/Polyethylene Glycol Composites from Gonggong Clam Shells for Efficient Rhodamine B Dye Removal. *Asian Journal of Green Chemistry*, 10 (3) 2026, 372-388.

DOI: https://doi.org/10.48309/AJGC.2026.550310.1840

URL: https://www.ajgreenchem.com/article_233169.html